Sugiura, Y. (1979a) *Biochem. Biophys. Res. Commun. 88*, 913.
Sugiura, Y. (1979b) *Biochem. Biophys. Res. Commun. 90*, 375.
Sugiura, Y., & Kikuchi, T. (1978) *J. Antibiot. 31*, 1310.
Sugiura, Y., Muraoka, Y., Fujii, A., Takita, T., & Umezawa, H. (1979) *J. Antibiot. 32*, 756.
Takahashi, K., Ekimoto, H., Aoyagi, S., Koyu, A., Kuramochi, H., Yoshioka, O., Matsuda, A., Fujii, A., & Umezawa, H. (1979) *J. Antibiot. 32*, 36.
Takeshita, M., Grollman, A. P., & Horwitz, S. B. (1976) *Virology 69*, 453.
Takita, T., Muraoka, Y., Nakatani, T., Fujii, A., Umezawa, Y., Naganawa, H., & Umezawa, H. (1978a) *J. Antibiot. 31*, 801.
Takita, T., Muraoka, Y., Nakatani, T., Fujii, A., Iitaka, Y., & Umezawa, H. (1978b) *J. Antibiot. 31*, 1073.
Umezawa, H. (1979) in *Bleomycin: Chemistry, Biochemistry and Biological Aspects* (Hecht, S. M., Ed.) p 24, Springer-Verlag, New York.
Umezawa, H., Maeda, K., Takeuchi, T., & Okami, Y. (1966) *J. Antibiot., Ser. A 19*, 200.
Umezawa, H., Hori, S., Sawa, T., Yoshioka, T., & Takeuchi, T. (1974) *J. Antibiot. 27*, 419.

Structure of Myosin Subfragment 1 from Low-Angle X-ray Scattering†

Robert Mendelson* and K. M. Kretzschmar

ABSTRACT: The X-ray scattering pattern produced by a solution of myosin subfragment 1 has been measured to a resolution (Bragg spacing) of 2 nm. We find that for subfragment 1 (S1) prepared by limited papain digestion in the presence of ethylenediaminetetraacetate the radius of gyration is 3.28 ± 0.06 nm, the volume is 151 ± 6 nm^3, the surface area is 330 ± 15 nm^2, and the length of the maximum chord is 12.0 ± 1.0 nm. The theoretical scattering patterns from several objects of uniform electron density have been calculated and compared with the observed scattering produced by S1. The recent three-dimensional electron micrograph reconstruction of S1-decorated actin by J. Seymour and E. O'Brien (private communication) generated the calculated pattern that best fit the observed scattering. This fit strongly suggests that this reconstruction resembles subfragment 1. The good correspondence between an S1 structure derived when S1 is attached to actin and a study of free S1 in solution strongly suggests that binding to actin does not grossly distort the shape of S1. This is consistent with the notion that S1 changes its orientation on actin, rather than its shape, in order to generate the contractile force in muscle.

The shape of the globular "head" portion of the myosin molecule (subfragment 1) has been a subject of considerable interest and controversy. Since the cross-bridges seen in electron microscopy of muscle consist primarily of these heads, even a low-resolution knowledge of their structure would greatly aid the analysis of X-ray diffraction by muscle fibers (Miller & Tregear, 1972; Squire, 1975; Lymn & Cohen, 1975; Haselgrove et al., 1976) and fluorescence polarization (Tregear & Mendelson, 1975; Mendelson & Morales, 1977) of muscle fibers. We report here the results obtained from low-angle X-ray scattering by the isolated subfragment 1 portion of myosin in solution.

Lowey et al. (1969) used rotary shadowing to establish that myosin has two "heads" and modeled these as spheres approximately 7 nm in diameter. Moore et al. (1970), studying the three-dimensional reconstruction of electron micrographs of negatively stained individual thin filaments "decorated" with subfragment 1 (S1),[1] found the heads to be asymmetric objects resembling a cupped hand. Similar results have been found by J. Seymour and E. O'Brien (private communication) on examining image reconstructions of S1 decorating thin filament paracrystals. Mendelson et al. (1973) found using fluorescence depolarization experiments that S1 in solution was elongate; when considered as a prolate ellipsoid of revolution, its axial ratio was 3.5 or greater. Other hydrodynamic measurements of Yang & Wu (1977) attributed an oblate shape to S1. Takahashi (1978), using a negative staining method on myosin, found that the heads were 21 nm long, while Elliott & Offer (1978) using a new rapid freeze rotary shadowing method found the heads of isolated myosin molecules to be about 19 nm long.

X-ray scattering from S1 in solution allows models to be tested with a resolution of up to 2 nm (Bragg spacing), and has the advantage that the shape is inferred from the native, enzymatically active particle.

In the first phase of this work, Kretzschmar et al. (1978) found that S1 had a radius of gyration of 3.24 nm, bearing out our earlier contention that the particle is quite asymmetric. Here we report wider angle (higher resolution) data, which permits us to select from among various proposed models of S1.

Materials and Methods

Protein Preparation. Myosin subfragment 1 was prepared from insoluble rabbit dorsal skeletal muscle myosin, using

† From the Cardiovascular Research Institute and the Department of Biochemistry and Biophysics, University of California, San Francisco, San Francisco, California 94143. *Received November 28, 1979.* This work was supported by U.S. Public Health Service Program Project Grants HL-16683 and HL-06285, National Science Foundation Grant PCM-75-22698, and in part by National Science Foundation Grant DMR 73-07692, in cooperation with SLAC and ERDA. We acknowledge use of the computer graphics facility at U.C.S.F., which was funded by National Institutes of Health Grant RR-1081.

[1] Abbreviations and symbols used: S1, subfragment 1 of myosin; fwhm, full width at half-maximum; $h = (4\pi/\lambda) \sin \theta$; λ, the X-ray wavelength; 2θ, the scattering angle; V, the molecular volume; S, the molecular surface area; R_g, the radius of gyration; LC1, LC2, and LC3, the light chains of myosin in descending order of molecular weight; BSA, bovine serum albumin; $NaDodSO_4$, sodium dodecyl sulfate; EDTA, ethylenediaminetetraacetate; Tes, *N*-tris(hydroxymethyl)methyl-2-aminoethanesulfonic acid; AMPPNP, adenylylimidodiphosphate.

0006-2960/80/0419-4103$01.00/0

insoluble papain as reported previously (Kretzschmar et al., 1978). Myosin was digested in the presence of 5 mM EDTA and purified by Sepharose G-200 gel chromatography. The yield of S1 was maintained at 10–15% in all preparations. The purified fraction (tubes within the central fwhm) was concentrated to 7–18 mg/mL by ultrafiltration in an Amicon concentrator and centrifuged at 140000*g* for 1 h. One preparation was made with Mg^{2+} present during digestion of myosin to check for the effect of increased uncleaved light chain 2 (LC2) retention (Margossian et al., 1975) on the scattering data.

The scattering experiments were performed at the Stanford Synchrotron Radiation Laboratory using the apparatus described previously. The data set used here includes some of the data reported previously. All measurements were made with S1 in a solution containing 0.15 M KCl and 10 mM Tes, pH 7, at 1 °C.

Comparison with Models. Models of S1 were computer constructed of 2500–3500 spheres of diameter 0.36–0.39 nm arranged in a face-centered cubic closest-packed configuration. All models had uniform electron density. Scattering patterns for these models were computed by using the Debye equation (1915) for the intensity, I, at scattering angle 2θ:

$$I(h) = \sum_i F_i \sum_j F_j \frac{\sin(hr_{ij})}{hr_{ij}} \quad (1)$$

where $h = (4\pi \sin\theta)/\lambda$, r_{ij} is the distance between the ith and jth spheres, and the Fs are spherical scattering factors. Tests with models for which the pattern could be calculated exactly from closed expressions showed that the accuracy of the computed intensity was always better than 1% (typically 0.1%) in the angular range that we considered. The scattering intensities computed for the models were convoluted with the beam-defining slit dimensions and the aperture height of the position-sensitive counter to allow comparison with observed data. The distance distribution (correlation) function was computed by Fourier transforming the deconvoluted data using the B-spline technique of Glatter (1976, 1977).

Results

Characterization of the S1 Preparations. The molecular weight was measured by comparing the scattering intensity (extrapolated to zero angle) with the corresponding intercept of bovine serum albumin (Armour, 3× crystallized). Taking the molecular weight of BSA (68 500) as a secondary standard, the molecular weight obtained for S1 was 109 000 ± 11 000. The error was estimated from the effect of possible BSA and S1 aggregation (estimated from the Guinier region), uncertainty in concentration measurement, and instrumental instabilities. Recently, Margossian & Stafford (1979) have shown that the molecular weight of S1 may be accurately determined by a measurement of the light chain content using NaDodSO$_4$–polyacrylamide gel electrophoresis. Because of the rather large error in the extrapolated zero angle measurement, we have also characterized our preparation by this method.

NaDodSO$_4$ gels revealed bands corresponding to a heavy chain (MW = 90 000) containing about 90% of the material of molecular weight greater than 20 000, a degraded heavy chain (MW ≈ 65 000), light chains, and a difference peptide from the heavy chain proteolysis. It was found that approximately 20% LC2 was retained uncleaved and a significant amount, ~45% (measured relative to LC3, which was not proteolyzed significantly), was found in a band of molecular weight 14 000. Studies of S1 gel patterns with varying degrees of myosin digestion showed that this band arises from LC2 proteolysis. Although the relative amount of degraded and intact LC2 (and LC1) varied somewhat from preparation to preparation, an average molecular weight of 121 000 ± 5000 was found. We assume no lighter peptides contribute to the molecular weight; in fact, no other bands of molecular weight greater than 7500 have been observed. This molecular weight is consistent with the work of Margossian & Stafford (1979), who found that S1 prepared in a similar manner has a molecular weight of 113 000 ± 3000 when isolated in an ion exchange column fraction in which the fragment of molecular weight 14 000 was absent (S. Margossian, private communication).

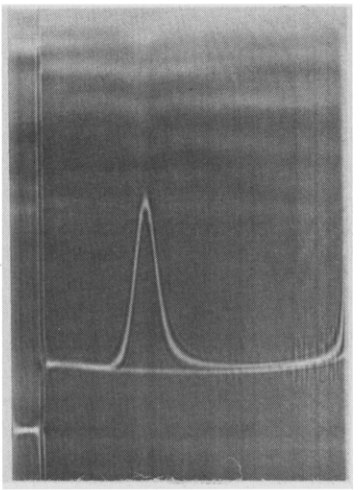

FIGURE 1: Sedimentation of an 18 mg/mL solution of column-purified S1 photographed after the hypersharp peak disappeared (t = 74 min). A small amount of heavy material could contribute to the rise seen at the extreme right. Samples were spun prior to X-ray exposure to remove any of this material. The rotor speed was 59 800 min^{-1} and the temperature was 4 °C.

In some trials aggregates were detected as a deviation from linearity in a Guinier plot (see also Kretzschmar et al. (1978)). For this reason the sedimentation of the preparation was studied in the analytical centrifuge. Studies of the sedimentation of the peak at different S1 concentrations gave a value of $s_{20,w} = 6.0 \pm 0.2 \times 10^{-13}$ s when extrapolated to zero concentration, in agreement with Lowey et al. (1969), who found $s_{20,w} = 5.8 \pm 0.1 \times 10^{-13}$ s. Few, if any, small aggregates were observed; however, some of the rise at the extreme right of the schlieren pattern could be due to material of high sedimentation coefficient (Figure 1). Consequently, all preparations were centrifuged at 140000*g* for 1 h prior to use to remove any large aggregates. The equivalence of molecular weights measured by NaDodSO$_4$ gel electrophoresis, extrapolated from zero-angle X-ray scattering and derived from molecular volume measurement using the entire X-ray scattering pattern (see below), supports the assertion that at most a few percent of the molecules are aggregated.

In order to study the possibility that otherwise undetectable aggregates may contribute to the data at larger angles, extensive modeling studies of the effect of a small degree of residual aggregation (dimers or larger up to 10% of the S1 concentration) showed that they would cause negligible distortion of the shape of the intensity curve for $hR > 1.2$. Furthermore, data from solutions containing aggregates, as ascertained by Guinier plots ($hR < 1.2$), was compared with data containing no discernible aggregates. No differences could be observed within statistical error.

Molecular Parameters. The data (Figure 2) were deconvoluted (Glatter, 1974) to eliminate slit width effects and were Fourier transformed to give the distance distribution (corre-

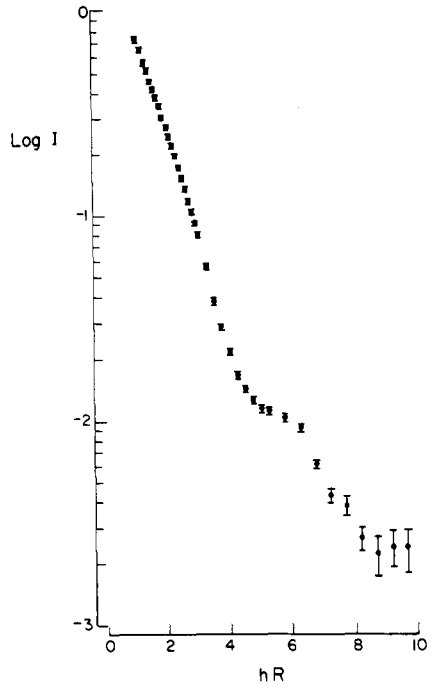

FIGURE 2: S1 scattering intensity as a function of angle. Here $hR = (4\pi R_g/\lambda) \sin\theta$, where θ is half the observed scattering angle and λ is the wavelength. Each data point is the mean calculated from data obtained in five different trials from three different preparations (7–8 mg/mL). The error bars are the standard deviations calculated from each set of five trials and therefore include all sources of random error.

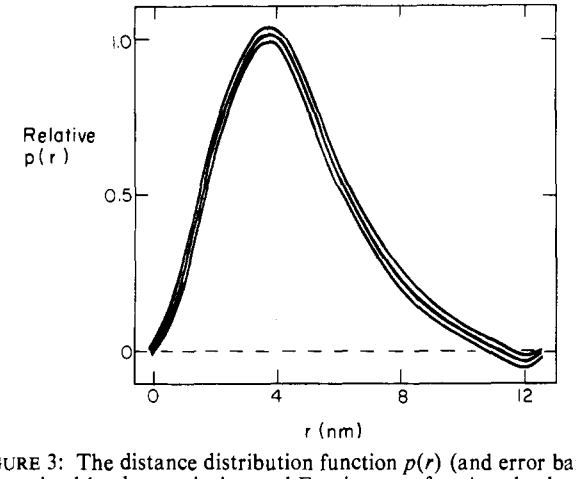

FIGURE 3: The distance distribution function $p(r)$ (and error band) determined by deconvoluting and Fourier transforming the data in Figure 2. The length of the maximum chord was determined to be 12.0 ± 1.0 nm (see text).

lation) function, $p(r)$, from which many molecular parameters were derived. Since $4\pi p(r)\,dr$ is the probability of an electron pair having a separation between r and $r + dr$, the longest chord, R_{max}, may be (ideally) obtained from the r intercept. Figure 3 shows the distance distribution function for S1. The small oscillation in the neighborhood of the maximum dimension is caused by residual concentration effects. Studies by Glatter (1979) show that the correct value of R_{max} is obtained at the minimum of the oscillation; hence, for S1 R_{max} = 12.0 ± 1.0 nm. Based on Glatter's work, the relative weakness of this oscillation allows us to conclude that these concentration effects are minimal and do not significantly distort the scattering pattern (all measured points, i.e., $hR > 1.05$, were included in the Fourier transformation). This is consistent with our finding that the scattering pattern at wide angles did not change significantly over a wide range of S1

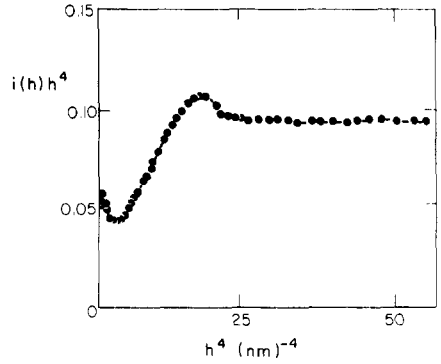

FIGURE 4: A Porod plot of $i(h)h^4$ vs. h^4 where $i(h)$ is the intensity corrected for slit smearing and normalized so that $i(0) = 1$. The largest abscissa value corresponds to a Bragg spacing of 2.3 nm. The area of S1 was obtained using the asymptote and eq 3 and 4.

concentrations from 7 to 18 mg/mL. This concentration insensitivity was to be expected, considering the previously reported insensitivity of the radius of gyration, which is a lower resolution measurement.

The radius of gyration, determined by eq 2, has a value of

$$R_g^2 = \frac{\int_0^\infty p(r) r^2\, dr}{2\int_0^\infty p(r)\, dr} \qquad (2)$$

3.28 ± 0.06 nm, which is slightly larger (1.2%) than we reported previously (Kretzschmar et al., 1978). The present analysis uses data obtained at both large and small angles and hence its deductions are model independent (and minimally aggregate dependent); some residual model dependence (ca. 1–3% under estimate of R_g) was conceded previously using only data in the Guinier region. Preliminary results using S1 prepared in the presence of Mg^{2+} and thus retaining more uncleaved LC2 show no significant difference in R_g from S1 prepared in the presence of EDTA.

Porod (1951) has shown that a necessary condition for having a scattering object of uniform electron density is that for large values of h the product $[i(h)][h^4]$ approaches a constant value. This limit is

$$\lim_{h\to\infty} [i(h)][h^4] = 2\pi S/V^2 \qquad (3)$$

where S is the surface area and V is the volume, and the intensity $i(h)$ is deconvoluted and normalized so that $i(0) = 1$. Thus, a plot of $i(h)h^4$ vs. h^4 should have zero slope for sufficiently large h; large deviations may be caused by nonuniformities in the protein electron density, residual concentration effects, or polydispersity (Murthy & Knox, 1977). Furthermore, if the electron density is uniform, as is the case for a typical globular protein, the volume may be computed from

$$V = 2\pi\left\{\int_0^\infty [I(h)]h^2\, dh\right\}^{-1} \qquad (4)$$

Since the Porod plot of the data (Figure 4) has a near zero slope, the volume and surface area were computed using eq 3 and 4 (see Table I). The primary source of error in S and V arises from the extrapolations of ih^2 (toward large angles) in the computation of V.

The measured value of V, 151 ± 6 nm^3, yields a molecular weight of 120 000 ± 5000 when the partial specific volume of 0.74 cm^3/g (from the amino acid composition; Yang & Wu, 1977) is used. The agreement with the molecular weight determined by NaDodSO$_4$ gel electrophoresis (121 000 ±

Table I: Properties of Subfragment 1

R_g (nm)	vol (nm^3)	$\bar{\nu}$ (mL/g)	max chord (nm)	surface area (nm^2)	$10^{13}s_{20,w}$ (s)
3.28 ± 0.06[a]	151 ± 6[a]	0.73[c]	12.0 ± 1.0[a]	330 ± 15[a]	5.8 ± 0.1[e]
	149 ± 6[b]	0.74[d]			6.0 ± 0.2[a]

[a] This work (see text). [b] Obtained using MW = 121 000 ± 5000 (from $NaDodSO_4$ gel electrophoresis) and $\bar{\nu}$ = 0.74 mL/g (see text). [c] See Sakura & Reithel (1972). [d] Amino acid composition. [e] Lowey et al. (1969). Other hydrodynamic properties have been tabulated by Yang & Wu (1977).

5000) is to be expected; since internal hydration in proteins is small and most of the electron density of the external hydration shell for proteins is near that of buffer (see, e.g., Richards, 1977), the X-ray scattering by solute-bound water alters the molecular weight by a negligible amount in comparison with the errors in our measurements.

Comparison with Models. Scattering curves produced by several models of subfragment 1, constrained to have a radius of gyration of 3.28 ± 0.06 nm and a volume of 151 nm^3 were computed using eq 1 (see Figure 5). With these constraints models such as oblate and prolate ellipsoids of revolution, spherical cones, rods, and circular cones with hemispherical caps have no adjustable parameters. Other models have additional parameters; for example, bent rods, elliptical cones with hemiellipsoidal caps, and ball plus stick models have one remaining degree of freedom. We have also computed scattering from a uniquely determined general ellipsoid using the further constraint of R_{max} = 12.0 nm. In comparing our data with shapes from electron microscopy in which the radius of gyration assumed by their authors was slightly different from the present X-ray scattering value (but the volume was the same), the ordinate (hR) values were computed using the appropriate electron microscopy value.

Scattering at small angles (small hR) corresponds to low spatial resolution. Therefore, the acceptability of a model is determined by the magnitude of the hR value at which its computed scattering curve first begins to deviate from the observed scattering pattern. The model which produces a scattering curve that fits the data to the largest scattering angle is considered best. As may be seen in Figure 5, none of the simple models, with the possible exception of a general ellipsoid, even begin to fit the data. Some simple models appear to give the correct overall scattering pattern; however, they must be excluded because of their poor fit at lower angles. A detailed statistical analysis of the fit was unnecessary, because the errors (see Figure 2) were small in comparison with the deviations of the fits obtained by simple models.

The three-dimensional reconstruction of electron micrographs of S1-decorated actin paracrystals was kindly furnished to us by J. Seymour and E. J. O'Brien (this reconstruction had the equator included at half-weight). No selection of their reconstructions was made by us. On the basis of a three-dimensional reconstruction of actin they ascertained the portion of the S1–actin micrograph belonging to S1. We have digitized their reconstruction, filled it with spheres, and scaled it to 151 nm^3 (and 139 nm^3) (see Figures 6A, 6B, and 6C). Scaling was necessary as the three-dimensional reconstruction technique generally underestimates the molecular volume. Uniform scaling (recommended by the authors) was accomplished by multiplying each coordinate by 1.184 (and 1.155). Other scaling methods, including scaling the x and y coordinates, but leaving the z (actin axis) dimensions unchanged, produced almost the same scattering pattern. With the volume scaled to 151 nm^3 (Figure 6E) as measured here, the radius

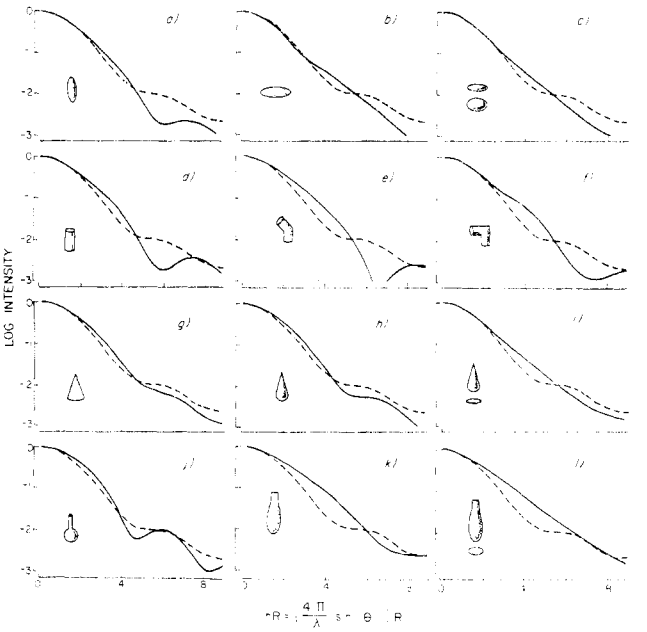

FIGURE 5: Fits of scattering from various uniform electron density models (—) to the data (---) using eq 1. Models are figures of revolution unless otherwise shown or stated. Models a through j are constrained by both the volume and the radius of gyration. Model c is a general ellipsoid additionally constrained by R_{max}; its semiaxes have lengths of 12.0, 7.9, and 3.1 nm. Models d, e, and f are rods with differing degrees of bend. Model g is a spherical cone. Model h is a cone with a hemiellipsoidal cap, and model i is the same except that it has an elliptical cross section with an axial ratio of 3. Models j, k, and l are taken from the electron microscopy of Elliott & Offer (1978) and Offer & Elliott (1978). In order to produce the correct radius of gyration in j, the rod portion was shortened and the radius of the spherical portion increased slightly to maintain the correct volume. Variations of these dimensions produced similar scattering curves (not shown). Models k and l are models presented by Offer and Elliott that have an elliptical cross section with axial ratios of 1 and 2, respectively.

of gyration was 3.20 nm, which differs from our measured value of 3.28 ± 0.06 nm by only 2%. The longest chord in the reconstruction was 12.1 nm, which also agrees closely with our measured value. In order to show the effect of error in the volume on the calculated scattering curve, the molecular volume derived from Margossian & Stafford (1979) (139 nm^3) (Figure 6D) was also used in the scaling of the micrographs. The radius of gyration was 3.12 nm and the scattering curve was little changed. Since this represents an extreme case, it can be safely stated that volume errors are unimportant for modeling purposes.

Discussion

We have compared scattering curves for many different shapes which various authors have used as models for S1. Of these the three-dimensional reconstruction of decorated thin filament paracrystals by J. Seymour and E. O'Brien (unpublished results) best fits the scattering data (Figures 6D and 6E).[2] The small remaining differences between their reconstruction and our data may be simply due to the slightly lower resolution of the micrograph reconstruction (about 3 nm) and/or to technique limitations rather than a significant change in tertiary structure between free and actin-bound S1. Of course, this shape may not be unique in its ability to fit

[2] The detailed coordinates of the reconstruction of Moore et al. (1970) were not available for comparison. However, the essential features of S1 shape in this reconstruction as published agree with those of the structure derived by J. Seymour and E. O'Brien (personal communication).

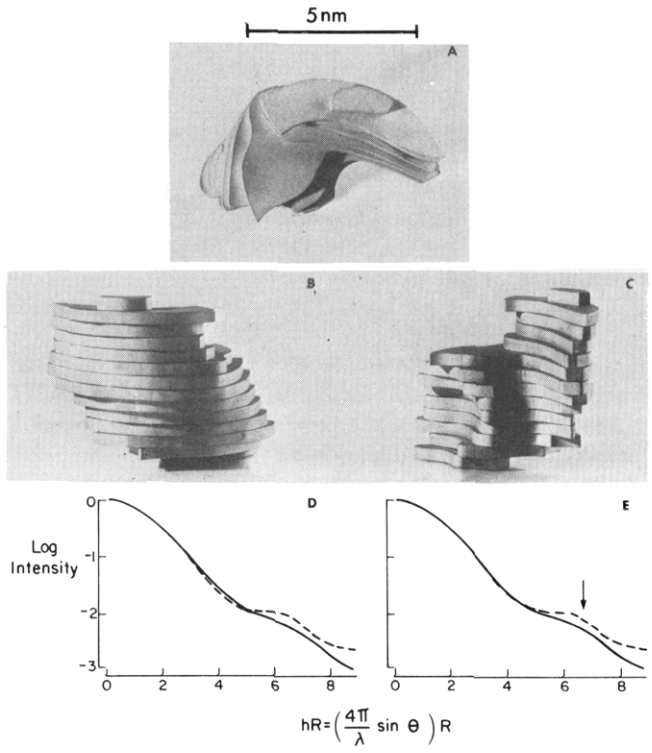

FIGURE 6: The three-dimensional reconstruction of J. Seymour and E. O'Brien (private communication) and its predicted X-ray scattering curves. (A) Top view looking down on the actin helix axis. (B and C) Side views looking (almost) transverse to the actin helix axis. The S1 is oriented so that the decorated actin–S1 complex would produce arrowheads pointing down the page. (D) The scattering curve (—) with the model volume scaled to 139 nm (MW = 113 000, $\bar{\nu}$ = 0.74 mL/g) and data (---). (E) The scattering curve with the model volume scaled to 151 nm^3 (as determined in this work). The scale in A (5-nm bar) is based on this later volume. Dimensions in B and C are to a different scale. They may be ascertained by noting that each layer is 0.59 nm thick. The arrow in E indicates the approximate resolution *(3 nm) of the electron micrograph reconstruction.*

the scattering data, since the phases of scattered X-rays are lost by spherical (solution) averaging. We (J. Chambers and R. A. Mendelson, unpublished results) are currently investigating the uniqueness question using a variation of the method of spherical harmonic decomposition of the mass density (cf. Stuhrman, 1977). However, the inability of a wide range of simple models to fit at even the lowest resolution makes it plausible that the reconstruction of Seymour and O'Brien contains realistic features of S1 up to ~3-nm resolution (Bragg spacing).

Although only the three-dimensional reconstruction gives a reasonable fit to the data, it is interesting that nearly all earlier work contains features of the model. For example, the silhouette of this model (cf. Figure 6B) appears roughly disk shaped in agreement with Lowey et al. (1969), yet the model has a low degree of symmetry, which would produce the significant hydrodynamic drag observed in fluorescence depolarization experiments. Also, the model contains a degree of oblateness as postulated by Yang & Wu (1977) and has the mass distribution skewed toward one end as suggested by Offer & Elliott (1978).

The longest chord in S1 is intermediate between the extremes of length suggested in the different experiments. If our result is applicable to S1 in a muscle fiber, then S1 is sufficiently long to span most of the interfilament distance (ca. 14 nm). Attachment to actin could then be accomplished by a relatively small amount of radial diffusion (see Mendelson & Cheung, 1976).

One enigmatic aspect of the three-dimensional reconstruction of S1 and actin is that it is quite difficult to understand how the heads can be helically arranged on actin and still be fastened to a common myosin rod in intact muscle. At this time there is conflicting evidence on whether each head of a given myosin binds to adjacent thin filaments or to the same filament (cf. Offer & Elliott, 1978). Since myosin and heavy meromyosin also decorate actin (with somewhat less regularity), either a large distortion must occur within the heads or there must be a small diameter stem (unseen at the resolution of those experiments) between S1 and the rod which is easily distorted (or both) if both heads bind to the same actin filament. (Fluorescence depolarization experiments (Mendelson et al., 1973) show that both heads can be simultaneously bound to some actin filament.) We are currently investigating this question.

Hydrodynamic and circular dichroism measurements (Gratzer & Lowey, 1969; Cassim & Lin, 1975; Mendelson et al., 1975) have shown that any conformational changes imposed by binding intact MgATP (simulated by MgAMP–PNP) or imposed by intermediates during ATP hydrolysis are small and do not alter the overall measurable molecular shape. Although these methods rely on certain assumptions (about the effect of label, circular dichroic interpretation, etc.), they are sensitive to alterations in the structure of unligated S1 at the resolution of the present work. Thus, it seems that S1 free in solution, ligated with nucleotide or not, has the same structure as when bound to actin (in the absence of nucleotide) to a resolution at least 4 nm. Assuming all of these findings apply in vivo, the present data lend support to the hypotheses (Reedy et al., 1965; Huxley, 1969; Huxley & Simmons, 1971) that S1 simply changes its orientation on actin during contraction rather than causing muscle to contract by a large change of S1 shape.

Acknowledgments

We are grateful to Dr. Jonathan Seymour and Dr. Edward O'Brien who furnished three-dimensional reconstructions of S1 prior to publication. We thank Dr. Gerald Offer who furnished a shape of S1 taken from electron micrographs of rotary-shadowed myosin prior to publication. We thank Professor Robert Langridge and the staff of the Computer Graphics Laboratory at the University of California, San Francisco, for their aid in digitizing these shapes. Several useful discussions with Dr. John Chambers, Professor Robert Langridge, Dr. Peter Moore, Dr. Robert Stroud, and Dr. Kenneth Taylor and helpful communications with Dr. Jonathan Seymour are gratefully acknowledged. We thank Professor Manuel Morales for many discussions and helpful comments throughout this work. Edward Giniger is gratefully acknowledged for his excellent technical assistance.

References

Cassim, J. Y., & Lin, T. I. (1975) *J. Supramol. Struct. 3*, 510–519.
Debye, P. (1915) *Ann. Phys. (Leipzig) 46*, 2927–2929.
Elliott, A., & Offer, G. (1978) *J. Mol. Biol. 123*, 505–519.
Glatter, O. (1974) *J. Appl. Crystallogr. 7*, 147–153.
Glatter, O. (1976) *Acta Phys. Austriaca 47*, 83–102.
Glatter, O. (1977) *J. Appl. Crystallogr. 10*, 415–421.
Glatter, O. (1979) *J. Appl. Crystallogr. 12*, 166–175.
Gratzer, W., & Lowey, S. (1969) *J. Biol. Chem. 244*, 22–25.
Haselgrove, J. C., Stewart, M., & Huxley, H. E. (1976) *Nature (London) 261*, 606–608.
Huxley, A. F., & Simmons, R. (1971) *Nature (London) 233*, 533–537.

Huxley, H. E. (1969) *Science 164*, 1356–1366.
Kretzschmar, K. M., Mendelson, R. A., & Morales, M. F. (1978) *Biochemistry 17*, 2314–2318.
Lowey, S., Slayter, H. S., Weeds, A. G., & Baker, H. (1969) *J. Mol. Biol. 42*, 1–29.
Lymn, R. W., & Cohen, G. H. (1975) *Nature (London) 258*, 771–772.
Margossian, S., & Stafford, W. (1979) *Biophys. J. 25*, 20a (Abstr.).
Margossian, S., Lowey, S., & Barshop, B. (1975) *Nature (London) 258*, 163–166.
Mendelson, R. A., & Cheung, P. (1976) *Science 194*, 190–192.
Mendelson, R. A., & Morales, M. F. (1977) *Biochim. Biophys. Acta 459*, 578–595 (Appendix).
Mendelson, R. A., Morales, M. F., & Botts, J. (1973) *Biochemistry 12*, 2250–2255.
Mendelson, R. A., Putnam, S., & Morales, M. F. (1975) *J. Supramol. Struct. 3*, 162–168.
Miller, A. M., & Tregear, R. T. (1972) *J. Mol. Biol. 70*, 85.
Moore, P. B., Huxley, H. E., & DeRosier, D. J. (1970) *J. Mol. Biol. 50*, 279–295.
Murthy, N. S., & Knox, J. R. (1977) *J. Appl. Crystallogr. 10*, 137–140.
Offer, G., & Elliott, A. (1978) *Nature (London) 271*, 325–329.
Porod, G. (1951) *Kolloid Z. 124*, 83–87.
Reedy, M. K., Holmes, K. C., & Tregear, R. T. (1965) *Nature (London) 207*, 1276–1280.
Richards, F. M. (1977) *Annu. Rev. Biophys. Bioeng. 6*, 151–176.
Sakura, J. D., & Reithel, F. J. (1972) *Methods Enzymol. 26*, 107–119.
Squire, J. M. (1975) *Annu. Rev. Biophys. Bioeng. 4*, 137–163.
Stuhrman, H. B. (1977) *Proc. Natl. Acad. Sci. U.S.A. 74*, 2316–2320.
Takahashi, T. (1978) *J. Biochem. (Tokyo) 83*, 905–908.
Tregear, R. T., & Mendelson, R. A. (1975) *Biophys. J. 15*, 455–467.
Yang, J. T., & Wu, C. C. (1977) *Biochemistry 16*, 5785–5789.

Alkyl Glycoside Detergents: A Simpler Synthesis and Their Effects on Kinetic and Physical Properties of Cytochrome *c* Oxidase†

Paul Rosevear,‡ Terrell VanAken, Jeffrey Baxter, and Shelagh Ferguson-Miller*

ABSTRACT: Octyl glucoside is an effective, nonionic, solubilizing agent for membrane proteins with the advantage of ease of removal by dialysis. In order to study the detergent-sensitive activity of cytochrome *c* oxidase, we chose this detergent because of its simple structure and the possibility of synthesizing analogues to test the structural dependence of the detergent specificity. A procedure was therefore developed that facilitates large-scale preparation of octyl glucoside and related alkyl glycosides, improving on previous methods by eliminating crystallization steps and employing a one-step purification of the final product on Dowex 1. This new purification procedure is particularly important for achieving the level of purity required to obtain the disaccharide, longer alkyl chain detergents in soluble form. Of the alkyl glycosides prepared (octyl β-D-glucopyranoside, octyl β-D-lactopyranoside, dodecyl β-D-lactopyranoside, dodecyl β-D-cellobiopyranoside, and dodecyl β-D-maltopyranoside), lauryl (dodecyl) maltoside was found to be the most successful as an activator of purified beef and *Neurospora* cytochrome oxidases, giving two- to tenfold higher activities than octyl glucoside and other commercially available detergents, Tween-20 and Triton X-100. Kinetic studies using two different steady-state assay systems indicate that the activity changes are not the result of altered binding of the substrate but rather reflect a detergent effect on the state of association of the enzyme (as a monomer, dimer, or polymer) as well as on its intrinsic activity. By gel filtration procedures, lauryl maltoside and octyl glucoside were found to exist as monodisperse populations of micelles of 50 000 and 8000 daltons, respectively. The small uniform micelles and chemically well-defined structures of lauryl maltoside and octyl glucoside make them superior to other nonionic detergents for the study of membrane proteins in general and cytochrome oxidase in particular, since its activity in lauryl maltoside most closely approaches that of the physiological state.

Octyl glucoside has recently been found to be an effective solubilizing agent for a number of membrane proteins (Baron & Thompson, 1975; Stubbs & Litman, 1978; Wittenberger et al., 1978; Felgner et al., 1979; Petri & Wagner, 1979). It is a small molecule of simple, defined structure which has a high critical micelle concentration that permits easy removal by dialysis. These properties have facilitated the purification and reconstitution of hexokinase-binding protein from mitochondrial outer membranes (Felgner et al., 1979), an isolation previously unattainable with numerous other detergents.

Mitochondrial cytochrome *c* oxidase has been isolated from many sources, but the electron transfer activity of the purified, multisubunit enzyme is found to be very sensitive to its detergent environment (Chuang & Crane, 1973; Yu et al., 1975; Robinson & Capaldi, 1977; Yu et al., 1979). It appears that the structure of the hydrophobic portion of the detergent is an important factor in the activity changes, but the kinetic characteristics and the molecular basis of the detergent effects have not been determined. With the ultimate aim of understanding the influence of membrane structure and other electron transfer proteins on cytochrome oxidase activity, the alkyl glycoside detergents were chosen to investigate the

† From the Department of Biochemistry, Michigan State University, East Lansing, Michigan 48824. *Received August 27, 1979; revised manuscript received April 15, 1980.* This work was supported by National Institutes of Health Grant GM 21731 to Dr. Robert Barker and National Institutes of Health Grant GM 26916-01 and Michigan State All-University Grant to S.F.-M.

‡ Present address: The Institute for Cancer Research, Fox-Chase, Philadelphia, PA 19111.

0006-2960/80/0419-4108$01.00/0